THE ASTROPHYSICAL JOURNAL, 448:623–627, 1995 August 1

NEGATIVE SEARCH FOR A COUNTERPART TO THE GAMMA-RAY REPEATER SOURCE 0525−66

JOHN R. DICKEL, YOU-HUA CHU, CHRISTOPHER GELINO, AND ROSS BEYER
Astronomy Department, University of Illinois, 1002 West Green Street, Urbana, IL 61801; johnd@astro.uiuc.edu, chu@astro.uiuc.edu, gelino@astro.uiuc.edu, rossb@astro.uiuc.edu

MICHAEL G. BURTON
School of Physics, University of New South Wales, Box 1, Kensington, NSW 2033, Australia; mgb@newt.phys.unsw.edu.au

D. K. MILNE
Australia Telescope National Facility, Box 76, Epping, NSW 2121, Australia; dmilne@atnf.csiro.au

JASON SPYROMILIO
European Southern Observatory, Karl-Schwarzschild-Strasse 2, 85748 Garching bei München, Germany; jspyromi@eso.org

DAVID A. GREEN
Mullard Radio Astronomy Observatory, Cavendish Laboratory, Madingly Road, Cambridge CB3 0HE, England, UK; dag@mrao.cam.ac.uk

CHRISTOPHER WILKINSON
Physics Department, University of Adelaide, Box 498, Adelaide, SA 5001, Australia; cwilkins@physics.adelaide.edu.au

AND

NORBERT JUNKES
Institut für Astronomie und Astrophysik, Universität Kiel, Olshausenstrasse 40, W-2300 Keil 1, Germany; supas050@astrophysik.uni-kiel.d400.de

Received 1994 December 27; accepted 1995 February 6

ABSTRACT

Radio continuum, near-infrared [Fe II], H_2, and Brγ, and optical Hα images of the supernova remnant N49 in the LMC, show a filamentary shell structure, characteristic of remnants in the adolescent or middle-aged phase of their evolution. No evidence is found in these images for any feature associated with the soft γ-ray repeater 0525−66 projected within the outline of this SNR. The nature of an X-ray hot spot located near the position of the γ-ray source remains uncertain, but the lack of emission at other wavelengths places significant limits on any nonthermal contribution to its radiation.

Subject headings: gamma rays: bursts — infrared: ISM: lines and bands — ISM: individual (N49, 0525−66) — supernova remnants

1. INTRODUCTION

The supernova remnant N49 was one of the first SNRs to be identified in the LMC (Mathewson & Healey 1964). Its bright, filamentary structure and fairly large size (diameter of ∼18 pc) suggests that it is in the adolescent stage of its development. It has swept up some tens of times the ejected mass, and the expansion can be modeled by the point-blast approximation (Sedov 1959). A super burst of cosmic γ-rays which occurred on 1979 March 5 was subsequently located inside the north-eastern edge of the SNR (Cline et al. 1980, 1982). A number of secondary bursts apparently from the same source occurred at least through 1983 (Golenetskii, Ilyinskii, & Mazets 1984). Recently detailed analyses of *Einstein* (Rothschild et al. 1993) and *ROSAT* (Rothschild, Kulkarni, & Lingenfelter 1994) high-resolution imager (RHRI) data on N49 revealed an X-ray hot spot within the γ-ray error box.

Images of N49 obtained by us at radio wavelengths with the compact array of the Australia Telescope, in the near-infrared with the Anglo-Australian Telescope, and at Hα from the *Hubble Space Telescope* (*HST*) archive program have been searched for evidence of a counterpart to this γ-ray burster. In the next section we describe the data and put upper limits on the emission from the position of this source in these wave bands. The results are discussed in § 3.

2. DATA

2.1. *Radio Continuum*

The radio data were obtained at a frequency of 2.378 MHz using four configurations of the compact array of the Australia Telescope with baselines extending out to 6 km. Absolute flux-density calibration was obtained from observations of PKS 1934−638, which had an assumed flux density of 16.2 Jy at this frequency. The spectrum and flux density of this source are tied to the scale of Baars et al. (1977). The secondary phase calibrator for position was PKS 0407−658, which had a positional accuracy of better than 0.″02 from VLBI measurements. The half-power beamwidth of the synthesized beam was 3.″0. The rms noise level on the map was 0.093 mJy beam^{-1}.

The radio image is shown in Figure 1. The SNR appears as an irregular shell with a diameter of about 75″ or 18 pc at the 49 kpc distance to the LMC (Feast 1991). The emission is much more prominent on the eastern side but does complete a full shell around the west. There is no feature visible within the error box of the γ-ray source (Cline et al. 1982), nor at the position of the X-ray hot spot at J2000 $05^h26^m00^s.7$ and −66°04′35″ (Rothschild et al. 1994). The latter positions are marked on Figure 2, which is the Hα image with selected contours from the radio image superimposed. The nearest radio

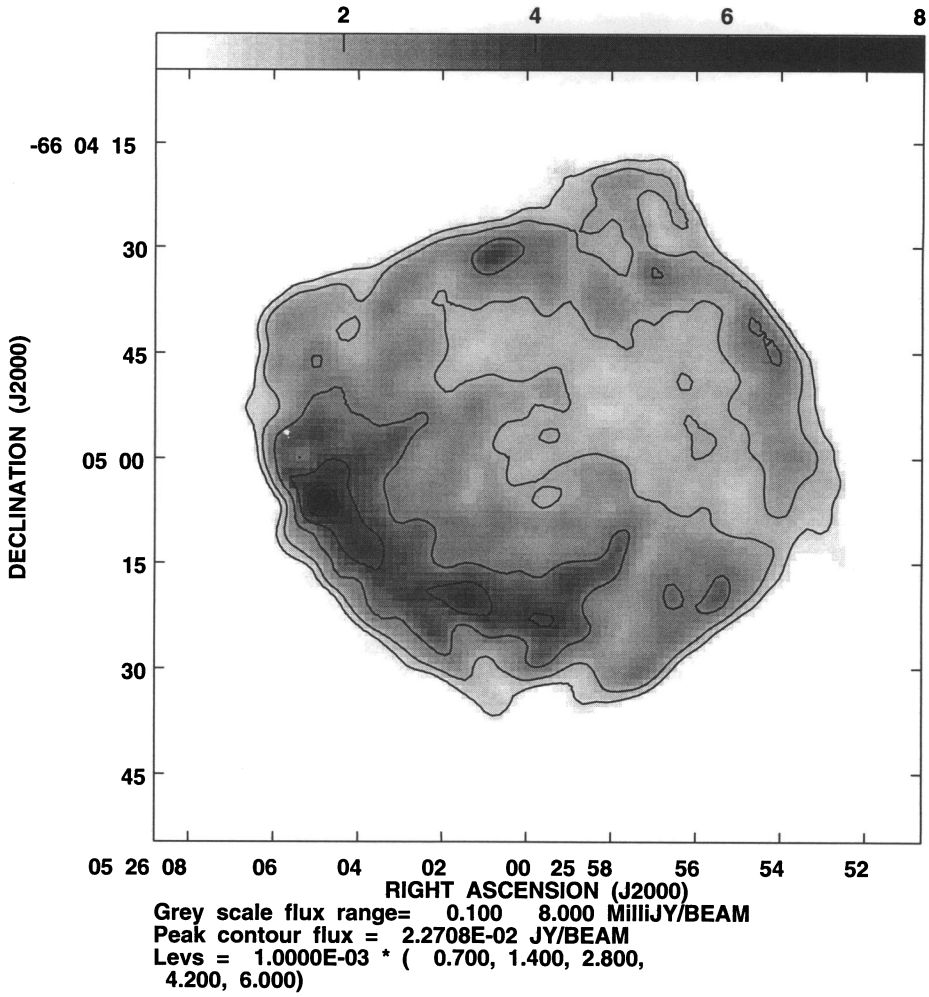

FIG. 1.—Continuum radio image of the supernova remnant N49 at a frequency of 2.378 MHz. Resolution is 3.″0.

feature to this position is about 5″ to the north and appears to be just the brightest part of a filament in the northern edge of the remnant. It coincides with the general shell structure of the X-ray emission in that region rather than the compact source. We therefore conclude that no compact radio source is present and give a 3 σ upper limit of 0.3 mJy for the flux density of any object.

2.2. *Infrared*

Images in the near-IR lines of [Fe II] at 1.64 μm, H_2 at 2.12 μm, and Brγ at 2.16 μm were obtained using the IR camera IRIS on the 3.9 m Anglo-Australian Telescope on 1993 January 4. The camera utilized a 128 × 128 HgCdTe Rockwell NICMOSII array. Using a 1% filter for each line, images were taken in a five-point cross, interleaved with sky frames, and then combined into a mosaic. Total on-source integration time per line was 5 minutes, and the array was read out nondestructively to improve the read noise. The image scale was 0.″6 pixel^{-1}, and the seeing was 1″. Flux calibration was made using the standard star HD 15189 (H = 8.159 mag and K = 8.126 mag). Contour plots of these images are shown in Figures 3, 4, and 5. We calculate the 1 σ line flux threshold to be 1.5 × 10^{-19} W m^{-2} arcsec^{-2} for the H_2 and Brγ lines and 2 × 10^{-19} W m^{-2} arcsec^{-2} for the [Fe II] lines. The 3 σ detection limit for a continuum point source (assumed to occupy 3 × 3 pixels) is 17.9 mag at 2.12 μm and 18.0 mag at 1.64 μm.

N49 has very strong [Fe II] emission at 1.64 μm. The [Fe II] morphology is virtually identical to that in Hα, indicating both that the lines are excited in the same regions and that the differential extinction across the source is small. Only weak H_2 and Brγ line emission is detected. This emission is at the location of the brightest parts of the [Fe II] image, and the morphology is again similar to that at Hα.

No compact sources are seen associated either with the position of the X-ray hot spot or with the peak of the radio emission. Near-IR line emission is present at the positions of both these sources, but it is clearly extended. Also, the diffuse line emission near the X-ray source is very weak and only evident in the [Fe II] image.

2.3. Hα

The Hα image was taken from the *Hubble Space Telescope* archive. It was a 1500 s exposure through the F656N filter for observation W0KT0101T with A. Davidsen as the principal investigator. Cosmic-ray removal was performed, and a gray-scale rendition of this image with selected radio contours superimposed is shown in Figure 2. There appears to be a discrepancy of almost 1″ in the positions of the optical and

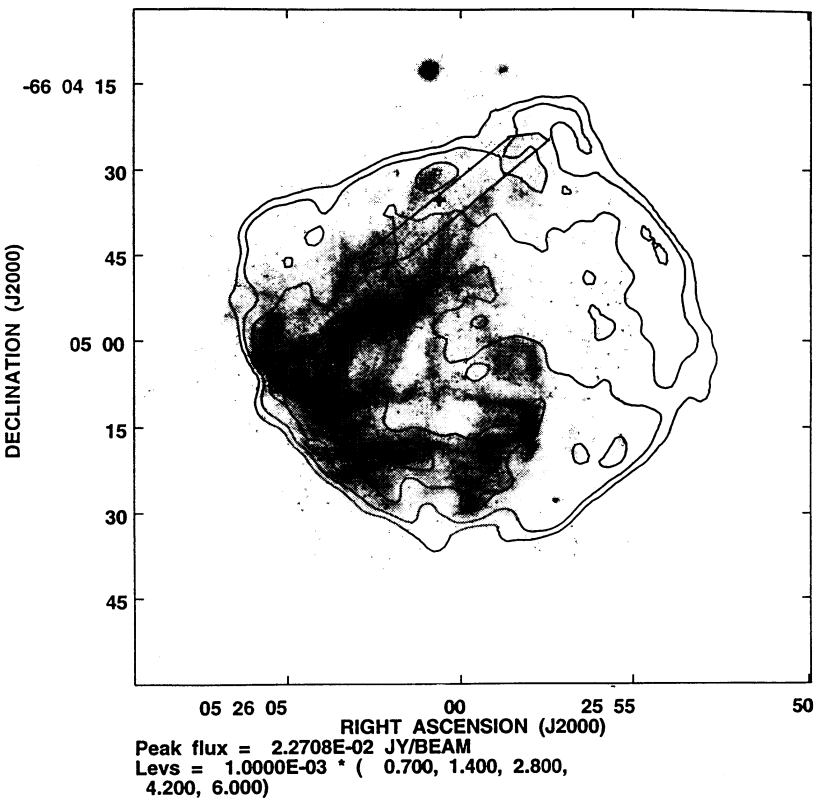

FIG. 2.—Hα image of the supernova remnant N49 from the *HST* archive with superimposed contours from the radio image. The error box of the γ-ray burst source is shown, and the cross marks the location of an X-ray hot spot.

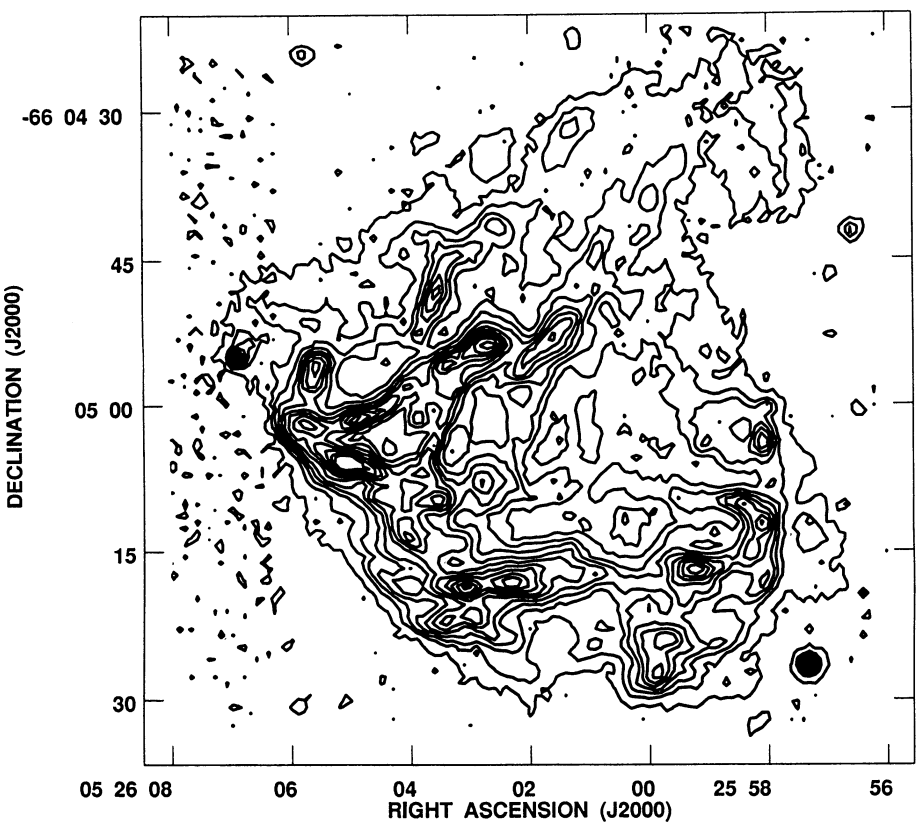

FIG. 3.—Contour map of the supernova remnant N49 in [Fe II] at 1.64 μm. Contours run from 2–52 × 10^{-19} W m^{-2} $arcsec^{-2}$ in increments of 5 × 10^{-19} W m^{-2} $arcsec^{-2}$.

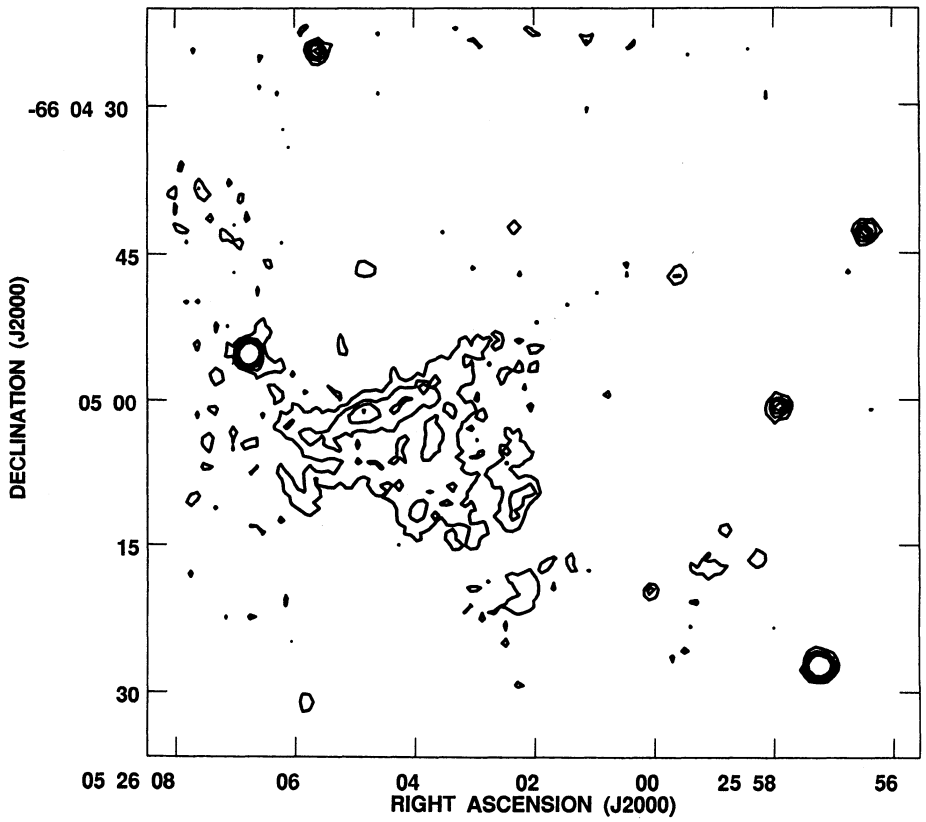

FIG. 4.—Contour map of the supernova remnant N 49 in H_2 at 2.12 μm. Contours are 1.5, 3, 4.5, 6, and 7.5 $\times$ 10^{-19} W m^{-2} arcsec^{-2}.

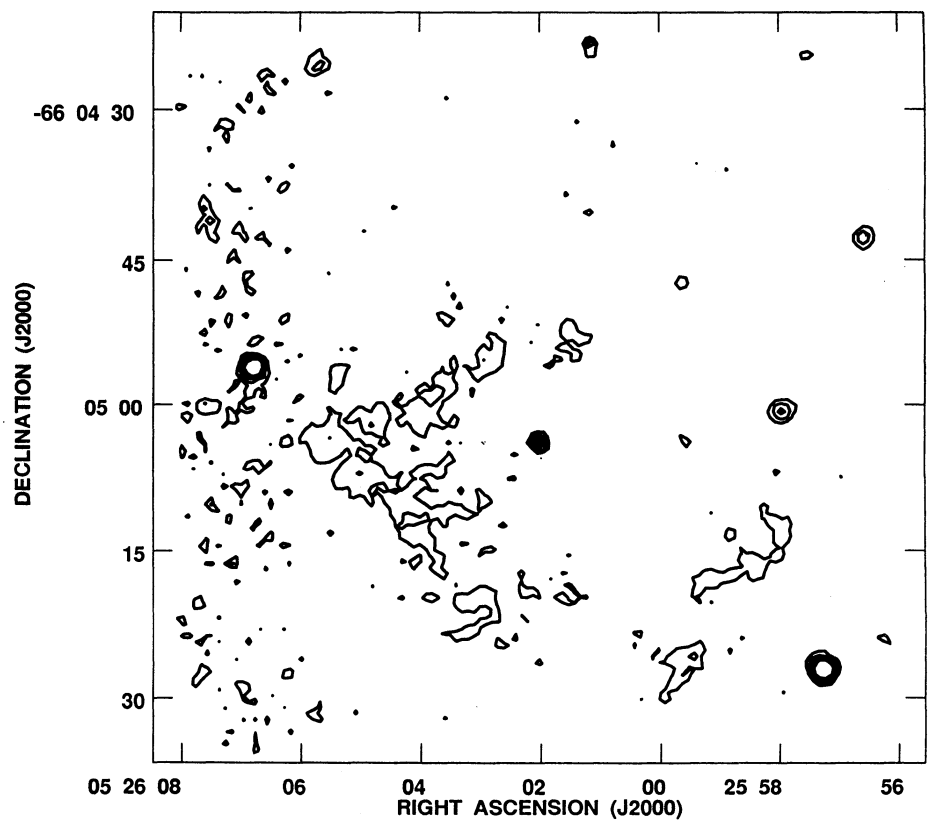

FIG. 5.—Contour map of the supernova remnant N49 in Brγ at 2.16 μm. Contours are 1.5, 3, 4.5, 6, and 7.5 $\times$ 10^{-19} W m^{-2} arcsec^{-2}.

radio images to get the best alignment between the observed features; this is significantly less than the uncertainty in the γ-ray and X-ray positions. The γ-ray error box is shown, and the location of the compact X-ray source is marked by the cross. Again, the filamentary structure of N49 is readily apparent in Hα, but no compact source is evident.

2.4. *X-Ray Data from the ROSAT Archives*

The image from the high-resolution imager shows a hot spot near the location of the γ-ray burster as indicated by Rothschild et al. (1994), but its size is difficult to determine with approximately 5″ resolution of the RHRI instrument. The Position Sensitive Proportional Counter, with a point spread function of about 30″, cannot resolve the hot spot but can give some modest spectral information. There is no indication of a change in the spectrum of the northern part of N49 containing the γ-ray source relative to the southern part. If the whole remnant is fitted to a Raymond-Smith thermal spectrum, the resultant temperature is 0.16 keV, and the absorbing column density along the line of sight is a high log $N_H = 22.0$. For normal adiabatic expansion, this temperature implies a shock velocity of 360 km s^{-1} which is very close to the value of 380 km s^{-1} found from echelle data measured toward several regions in the SNR, including the X-ray hot spot by Chu & Kennicutt (1988). Thus, the hot spot, which provides 2%–3% of the total X-ray luminosity of the SNR, could be a thermal feature. If so and if it has a filling factor of 1.0 within a radius of 5″, the mean density of the clump would be 160 cm^{-3}.

3. DISCUSSION AND CONCLUSIONS

The new images in all three wavelength bands appear virtually identical, with a one-to-one correspondence of the individual filaments. This structure is characteristic of adolescent and older SNRs which have entered the point-blast (Sedov 1959) phase of their evolution (e.g., Mufson et al. 1986; Straka et al. 1986). The bright filaments are probably clouds which were compressed by the shock passage and have subsequently cooled. There is also no indication of any wakes or other structures associated with a moving neutron star such as found in several SNRs with pulsar associations (e.g., Becker & Helfand 1985).

The upper limits to the flux densities of the compact X-ray source in N49 are presented in Table 1, along with the flux density derived from the X-ray luminosity of 7×10^{35} ergs s^{-1} given by Rothschild et al. (1994). It is difficult to predict the expected intensity of this source at the longer wavelengths unless its spectrum is known. If it is a synchrotron source surrounding a pulsar, then we can use the Crab Nebula and the central component of the composite remnant 0540−693 in the LMC as analogs. The complete spectra of both these objects are shown and compared by Manchester, Staveley-Smith, & Kesteven (1993). We note that the two comparison sources have somewhat different spectra. Although they have almost the same flux density at radio wavelengths, the radio emission of the Crab Nebula is 10 times brighter than that of the filled-center compact component which surrounds the pulsar of 0540+693.

TABLE 1

CONTINUUM FLUX DENSITY LIMITS FOR THE GAMMA-RAY BURSTER 0525−66

Wavelength (or energy)	Flux Density (Jy)
12.6 cm	<0.3
2.16 μm	$<3.9 \times 10^{-5}$
1.64 μm	$<5.8 \times 10^{-5}$
656.3 nm	$<4 \times 10^{-5}$
0.1–2.4 keV	4.4×10^{-7}

Clearly, if N49 has a nonthermal compact component, it must have a much flatter spectrum than even the feature in 0540−693. While the spot in N49 is about 1/10 as bright as 0540−693 in X-rays, it is $<1/100$ in the infrared and $<1/300$ in the radio. Maintenance of such a large fraction of high-energy X-ray–producing electrons would require a very low age of perhaps 1000 yr for this remnant (see Green & Scheuer 1992), which is considerably less than expected for its size and morphology. Thus, the X-ray emission from the hot spot on the north edge of N49 is likely not synchrotron radiation from a Crablike component.

Alternatively, the X-ray emission could be thermal bremsstrahlung from a dense clump of gas heated by passage of the SNR shock. In this case, we would expect the X-ray emission to have a general resemblance to the radio, optical, and infrared emission. This is observed for the other features in the shell, but not for the X-ray hot spot.

We therefore conclude that there is no indication at other wavelengths of the X-ray hot spot proposed as the counterpart of the repeating γ-ray burster within the outline of the SNR N49. It is impossible to measure ages of SNRs, but its morphology and size indicate that N49 is adolescent with an age of a few thousand years. If the X-ray and γ-ray source was responsible for the supernova, then, as stated by Rothschild et al. (1994), the object must have a transverse velocity of about 1200 km s^{-1}, which is high. It should also have left some morphological signature in the remnant. The X-ray source may therefore have a hard spectrum and be the compact accreting binary or other source of the γ-ray bursts, but its association with N49 is very doubtful.

Partial financial support was provided by US NSF grant INT 91-14551 and NASA grant HST-AR-5295.01-93A.

REFERENCES

Baars, J. W. M., Genzel, R., Pauliny-Toth, I. I. K., & Witzel, A. 1977, A&A, 61, 99
Becker, R. H., & Helfand, D. J. 1985, Nature, 313, 115
Chu, Y. H., & Kennicutt, R. K. 1988, AJ, 95, 1111
Cline, T. L., et al. 1980, ApJ, 237, L1
———. 1982, ApJ, 255, L58
Feast, M. W. 1991, in The Magellanic Clouds, ed. R. F. Haynes & D. K. Milne (Dordrecht: Kluwer), 1
Golenetskii, S. V., Ilyinskii, V. N., & Mazets, E. P. 1984, Nature, 307, 41
Green, D. A., & Scheuer, P. A. G. 1992, MNRAS, 258, 833
Manchester, R. N., Staveley-Smith, L., & Kesteven, M. J. 1993, ApJ, 411, 756
Mathewson, D. S., & Healey, J. R. 1964, in The Galaxy and the Magellanic Clouds, ed. F. J. Kerr & A Rodgers (Canberra: Australian Acad. Sci.), 283
Mufson, S. L., McCollough, M. L., Dickel, J. R., Petre, R., White, R., & Chevalier, R. A. 1986, AJ, 92, 1349
Rothschild, R. E., Kulkarni, S. R., & Lingenfelter, R. E. 1994, Nature, 368, 432
Rothschild, R. E., Lingenfelter, R. E., Seward, F. D., & Vancura, O. 1993, in Compton Gamma-Ray Observatory, AIP Conf. Proc. No. 280, ed. M. Friedlander, N. Gehrels, & D. Macomb (New York: AIP), 808
Sedov, L. 1959, Similarity and Dimensional Methods in Mechanics (New York: Academic Press)
Straka, W. C., Dickel, J. R., Blair, W. P., & Fesen, R. A. 1986, ApJ, 306, 266